Am J Transl Res 2022;14(9):6484-6503
www.ajtr.org /ISSN:1943-8141/AJTR0143910

Original Article

Biological functions of RNA modification patterns that define tumor microenvironment and survival outcomes in testicular germ cell tumors

Weijun Tang*, Jinke Qian*, Shilei Qian

*Department of Urology, Binhai People's Hospital, Yancheng 224500, Jiangsu, China. *Equal contributors.*

Received May 4, 2022; Accepted August 12, 2022; Epub September 15, 2022; Published September 30, 2022

Abstract: Background: Accumulating evidence has indicated that aberrant RNA modifications are associated with malignant progression and the immune microenvironment in various tumors. However, the function of RNA modification regulators in testicular germ cell tumors (TGCTs) remains to be discovered. This study aimed to investigate the biological functions of RNA modification regulators in testicular germ cell tumors and identify their potential clinical predictive value. Methods: Expression level of 75 RNA modification regulators was acquired to generate differential expression patterns. RNA modification regulatory genes were applied to construct a progression-free survival (PFS) risk model. Meanwhile, three RNA modification clusters were identified using consensus clustering. Subsequently, the infiltration characteristics of cells in the microenvironment as well as the antitumor drug candidates have been further analyzed. Finally, to further validate our results, we examined the expression and biological behavior of seven selected RNA modification regulators both in TGCT cell lines and clinical tissues. Results: We collected the differentially expressed regulators of RNA modification. RNA modification risk signature was developed to stratify the prognosis of TGCT patients. Furthermore, we found significant differences in immune microenvironment between subgroups. Ultimately, seven selected RNA modification regulators were further verified. Conclusions: We generated and validated a risk signature related to RNA modification which could accurately predict the relapse risk in TGCT patients. This risk signature was correlated with immune cells infiltration among tumor microenvironments. Furthermore, we screened antitumor drug candidates and evaluated the sensitivity and efficacy of class chemotherapeutic drugs, which could provide reference for clinical drug use.

Keywords: RNA modification risk signature, testicular germ cell tumor, immune microenvironment, anti-cancer drugs, bioinformation analysis

Introduction

Testicular germ cell tumors are the most common solid malignancy among young men aged from 15 to 40, which accounts for 90% of primary testicular tumors. They are broadly classified into two main pathological types, including seminoma and non-seminoma [1-3]. In detail, TGCTs can be histologically classified into seminomas (SEs) or the heterogeneous family of non-seminomas (NSs), the latter including embryonal carcinoma (EC), choriocarcinoma (CH), yolk sac tumor (YST), and teratoma (TE) subtypes, as well as mixed tumors (comprising mixtures of several components) [4]. Generally, non-seminoma's onset age is much younger than seminoma's [5]. Testicular germ cell tumors are often considered to be highly treatable and curable. Surgery, radiation therapy, chemotherapy, or stem cell transplantation are some of the mainstream treatments [1, 6]. Nevertheless, the major clinical challenges in this field remain to be overcome. Approximately 15-30% of TGCT patients will relapse after first-line chemotherapy [7]. Meanwhile, the side effects of chemotherapy cannot be ignored, such as cerebrovascular accidents [8]. Therefore, it is crucial to identify effective biomarkers for early diagnosis, monitoring disease progression and identifying promising therapeutic intervention targets.

So far, over 100 different RNA modification patterns have been reported [9]. The major RNA

modifications consisted of m1A, m3C, m5C, m6A, m7G, Nm modification, Pseudouracil (ψ), APA modification, and A-I modification [10]. RNA modification not only affects protein synthesis by modifying mRNA, tRNA and rRNA indirectly, but also affects gene expression through non-coding RNA directly [11, 12]. Although RNA modification regulators are not considered to be the driving genes of cancer, they can regulate RNA metabolism and affect the rate of protein synthesis, and participate in the progression of the majority tumors [13]. Each RNA modification is mainly divided into three classes: "writer", "reader" and "eraser", which is a kind of dynamic reversible process. It has been widely reported that m6A modification includes "writers" (METTL3, METTL14, WTAP, VIRMA, RBM15 and ZC3H13), "erasers" (FTO and ALKBH5), and "readers" (YTHDC1, YTHDC2, YTHDF1, YTHDF2, YTHDF3, IGF2BP1, IGF2BP2 and IGF2BP3) [14-16]. The regulatory factors responsible for m5C modification of RNAs include NSUN1 to NSUN7 and DNA methyltransferase-like 2 (DNMT2) [17]. Furthermore, it has been revealed that some m6A modification enzymes are also responsible for the modification of m1A, such as YTHDF1, YTHDF2 and YTHDF3 [9]. Gonçalves et al. confirmed that the m6A regulator VIRMA is involved in tumor progression, DNA damage response and cisplatin resistance in germ cell tumors [18]. However, overwhelming evidence has concentrated on the influence of single RNA modifications and lacked integrative analysis towards multifarious RNA modifications. The comprehensive analysis of multiple RNA modifications in TGCT remains to be elucidated.

In this study, we aimed to illustrate the correlation and biological function of the RNA modifications among TGCT patients. We first identified the differential RNA modification regulators expression level from TCGA and GTEx database, and respectively assessed among the types of RNA modifications. We then selected seven RNA modification regulators to develop a risk signature to predict progression-free survival in TGCT patients. Meanwhile, we validated the specificity and sensitivity of the risk signature model and estimated its therapeutic and prognostic value. We revealed that RNA modification regulatory factors were associated with the tumor immune environment and immune checkpoints response. Finally, we estimated the sensitiveness of chemotherapeutic agents and screened out candidate small molecular compounds for guiding clinical interventions.

Materials and methods

TGCT patients' data acquisition

Gene expression matrix (FPKM format), somatic mutation and SCNAs data which contain 165 normal tissues and 156 tumor samples, together with matched clinical and survival information were downloaded from TCGA and GTEx database (Version 8).

PPI network and correlation analysis

STRING database was applied to construct the protein-protein interaction (PPI) network. Cytoscape and Metascape website was further applied to visualize the PPI network. Moreover, spearman correlation analysis was performed to evaluate the interaction among these regulators. Consensus clustering analysis was employed to classify the TGCT samples into distinct subgroups.

Development and validation of an RNA modification-related prognostic signature

To screen out prognostic RNA modification-related genes, we applied multi-variate cox analysis to construct a prognostic signature. The RNA modification-related risk signature was calculated as follows:

$$\text{RNA modification Risk Signature} = \sum_{i=0}^{n}\left(\text{Exp(i)} * \text{Coef(i)}\right)$$

Where the Exp(i) and Cofe(i) represent the expression level of each gene and risk coefficients.

Kaplan-Meier survival curves were employed for revealing whether the risk score can differentiate the PFS in TGCT patients. Notably, we verified the prediction performance and stability of this prognostic signature in the testing cohort and the entire cohort.

Evaluating component of immune cell infiltration in immune microenvironment

To exhibit the complex components of the immune cell infiltration landscape, we conducted several algorithms, including XCELL [19, 20],

TIMER [21, 22], QUANTISEQ [23, 24], MCPCOUNT [25], EPIC [26], CIBERSORT [22, 27] and CIBERSORT-ABS [28] to estimate the subpopulations of immunity infiltration scores. Immune checkpoint-related genes were achieved from Auslander et al. [29].

Prediction of response to potential chemotherapy drugs

"pRRophetic" was used to gather information on estimate half maximal inhibitory concentration (IC50) of common chemotherapeutic drugs for patients with testicular germ cell tumor [30]. Meanwhile, Connectivity Map dataset (CMap; https://clue.io/) was applied to discover potential small molecular compounds. Finally, these candidate compounds' 3D structure tomographs were acquired from PubChem website (https://pubchem.ncbi.nlm.nih.gov), respectively.

Cell culture and qRT-PCR

The testicular germ cell tumor cells (Tcam-2) and Human testis cells (Hs 1.Tes) were cultured in DMEM (Biological Industries, BI, Israel) which contained 10% certified fetal bovine serum (VivaCell, Shanghai, China). Tcam-2 cells were transfected with control siRNA and siRNA-ADARB1 using Lipofectamine 3000 (Invitrogen, Thermo Fisher Scientific, USA).

Total RNA was isolated with Trizol reagent (Invitrogen, USA). HiScript II RT SuperMix (Vazyme, China) was used for cDNA synthesis. qRT-PCR was performed with SYBR qPCR Master Mix (Vazyme, China) using LightCycler 480 (LC480) real-time PCR instrument (Roche, Switzerland). The primers and siRNA oligo used in this study were listed in Table S1. Relative mRNA expression level was calculated using the $2^{-\Delta\Delta Ct}$ method and normalized against β-actin.

Cell proliferation and migration assays

Cell proliferation was measured after 24 h, 48 h, 72 h, and 96 h using Cell Counting Kit-8 (CCK-8, MedChemExpress, China). The absorbance was measured following incubation at 37°C for 1 h according to the manufacturer's protocols.

For the colony formation assay, pretreated cells were incubated for 10 days, then fixed in 4% paraformaldehyde for 20 min, and stained with 0.1% crystal violet for analysis.

A total of 1.5×10^5 cells were seeded into the 24-well Transwell chambers with serum-free medium for the migration assays. Medium containing 20% FBS was added to the bottom chamber. After incubation at 37°C for 48 hours, cells were fixed, stained, and captured with microscope.

Clinical samples and immunohistochemistry (IHC)

Seminoma clinical tissues were acquired by radical orchiectomy. All patients involved understood and signed the informed consent. This research was approved by the Ethics Committee of Binhai People's Hospital. IHC staining was performed by the Department of Pathology, Binhai People's Hospital. Briefly, the primary antibody was incubated as: anti-ADARB1 (Proteintech, 1:200, China).

Statistical analysis

Statistical data were processed by R 4.1.2 software. Then, we filtered out differential expression genes (DEGs) according to the false discovery rate (FDR) adjusted *P*-value <0.05 and $\log_2|\text{fold change}| > 0.5$ between the TGCT tumor samples and normal samples using Wilcoxon's test. The correlation analysis among RNA modification regulators was carried out by Spearman correlation analysis. Wilcoxon test was used to compare the distribution of immune cells in different risk subgroups. The chi-square test was performed to evaluate the association between the risk score and clinicopathological parameters. Functional enrichment terms with q-value <0.05 was considered significantly enriched. Kaplan-Meier survival analysis was carried out to evaluate survival predictive performance. The results with two-side *P*<0.05 were considered statistically significant.

Results

Expression and mutation landscape of RNA modifications regulators in TGCT

Firstly, based on the published reports, a total of 75 RNA modification regulatory factors and matched clinical information were enrolled in this current study [31] (**Table 1**). After filtration

Table 1. Summary of RNA adenosine modification regulators

RNA modification types	Major regulators
m1A	TRMT6, TRMT10C, BMT2, RRP8, TRMT61A, TRMT61B, ALKBH1, ALKBH3, YTHDF1, YTHDF2, YTHDF3, YTHDC1
m3C	METTL2A, METTL2B, METTL6, METTL8
m5C	NSUN2, NSUN3, NSUN4, NSUN5, NSUN6, NSUN7, NOP2, DNMT1, DNMT3A, DNMT3B, TRDMT1, ALYREF, YBX1, TET2, TET3
m6A	METTL3, METTL14, RBM15, RBM15B, METTL16, WTAP, ZC3H13, METTL5, CBLL1, VIRMA (KIAA1429), ZCCHC4, YTHDC1, YTHDC2, YTHDF1, YTHDF2, YTHDF3, HNRNPA2B1, IGF2BP1, IGF2BP2, IGF2BP3, ABCF1, FMR1, PRRC2A, ELAVL1, RBMX, LRPPRC, ALKBH5, FTO
m7G	METTL1, WDR4
Nm modification	FTSJ1, TRMT44
Pseudouracil (ψ)	PUS7
APA modification	CPSF1, CPSF2, CPSF3, CPSF4, CSTF1, CSTF2, CSTF3, CFI, PCF11, CLP1, NUDT21, PABPN1
A-I modification	ADAR, ADARB1, ADARB2

depending on adj. P<0.05 and $\log_2$|fold change| >0.5, a total 53 differential RNA modification regulators were screened out, of which 38 genes were up-regulated and 15 genes were down-regulated (**Figure 1A**). All differently expressed RNA modification regulators were listed in **Table 2**. Cluster heatmap and boxplot were utilized to visualize the expression profiles of 53 differential RNA modification regulators, including m1A, m3C, m5C, m6A, m7G, Nm modification, Pseudouracil (ψ), APA modification, A-I modification (**Figure 1B**, **1C**). In conclusion, our findings revealed that the expression levels of most RNA modification regulators were significantly distinct between tumor tissues and adjacent normal samples (**Figure 1A-C**).

Additionally, Genetic alteration information of RNA modification regulators was explored employing on TCGA-TGCT cohort (Figure S1A) and cBioPortal database [32] (Figure S1C) to discover the potential influence of genetic alterations upon the corresponding gene expression. The location of CNV alteration of RNA modification regulators on chromosomes was shown in Figure S1B. Through the investigation of CNV frequency, we found that CNV alterations in 75 regulators were prevalent, and the vast majority were concentrated on the gain in copy number [21, 33] (Figure S1D). Taken together, we found that NOP2 and CPSF1 had the highest genetic alteration and highest frequency of copy number variation.

Analysis of RNA modification-related signal pathways

To better understand the functional implication of 53 differentially expressed RNA modification regulators, functional enrichment analysis was performed, respectively. In accordance with the total DEGs, the association with the biological process included RNA methyltransferase; cellular components included methyltransferase complex, and nuclear speck; molecular function included methylation, RNA modification and ncRNA processing (**Figure 2A**, **2B**). KEGG analysis identified enrichment for: mRNA surveillance pathways, MicroRNAs in cancer, and Spliceosomes (**Figure 2C**, **2D**).

Interaction among RNA modifications regulators and functional enrichment

To better discover the relationship among RNA modifications regulators, we calculated the pairwise interaction correlations among 53 RNA modification regulators. We investigated that the expression of RNA modification regulators was markedly correlated and found that they share a high correlation in expression level (**Figure 3A**). Meanwhile, there was a strong correlation between the transcriptional level of these genes (**Figure 3B**). Next, we constructed PPI network using STRING database and visualized by Cytoscape software (**Figure 3C**). Furthermore, we performed cluster analysis via Metascape website to identify the biological functions of these distinct RNA modification

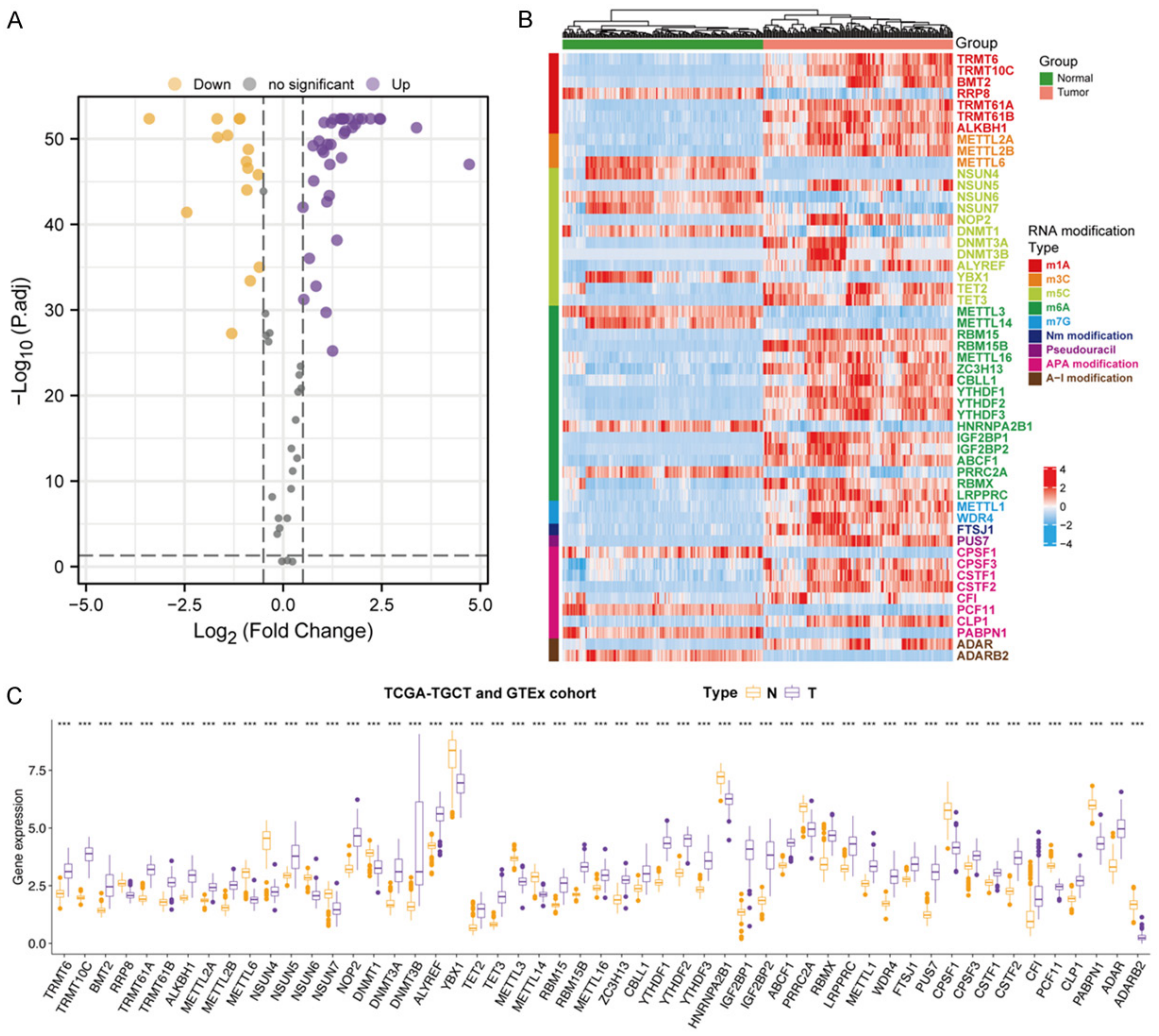

Figure 1. The landscape of expression patterns of RNA modification regulators between TGCT samples and normal tissues. A. A volcano plot generated with FDR<0.05 and $\log_2|FC|>0.5$, using the data of differentially expressed RNA modification regulators in TGCT downloaded from TCGA and GTEx databases. B. Hierarchical clustering of TGCT and normal tissues differentially expressing 53 RNA modification regulators. C. The expression of selected 53 RNA modification regulators between TGCT and normal tissues. Purple represents tumor group and yellow represents normal tissue group. TCGA, The Cancer Genome Atlas; GTEx, Genotype-Tissue Expression. *, P<0.05; **, P<0.01; ***, P<0.001; ns, no significant.

regulatory factors, which were remarkably focused on RNA modification, ncRNA processing and metabolism of RNA (**Figure 3D**). Ultimately, we extracted four modules using plug-in MCODE in Cytoscape. The four highest enrichment sub-modules were illustrated in **Figure 3E**. Consequently, crosstalk of RNA modification patterns may be important for the generation of different subtypes of individual TGCT tumors.

Consensus clustering analysis distinguished three TGCT subtypes

To further validate RNA biological function, we performed consensus clustering analyses based on these differently expressed RNA modification regulators. Clearly, the most suitable k-index was 3, namely. Thus, we distinguished a total of 156 samples into three distinct RNA modification patterns using unsupervised clustering, including Cluster A, B and C (**Figure 4A-C**). Moreover, principal component analysis (PCA) was performed for comparison of the expression profile (**Figure 4D**). Next, the results from GSVA enrichment analyses have revealed that significantly different pathways were activated among the three RNA modification Cluster. RNA modification cluster B was significantly enriched in p53 signaling pathway and fatty acid metabolism compared with clus-

Table 2. Fifty-three differentially expressed RNA modification regulator genes were identified from TGCT patients, including 38 up-regulated genes and 15 down-regulated genes

DEGs	Genes
Up-regulated genes	ADARB2, NSUN4, PABPN1, CPSF1, METTL6, YBX1, METTL3, PCF11, HNRNPA2B, PRRC2A, METTL14, NSUN6, NSUN7, RRP8, DNMT1.
Down-regulated genes	CSTF1, CPSF3, METTL16, METTL2A, FTSJ1, CBLL1, METTL1, CLP1, ZC3H13, ABCF1, NSUN5, LRPPRC, TRMT61B, RBMX, TRMT6, RBM15, ALKBH1, CFI, METTL2B, TET2, RBM15B, ALYREF, TRMT61A, YTHDF3, YTHDF2, WDR4, NOP2, BMT2, CSTF2, ADAR, DNMT3A, YTHDF1, TET3, TRMT10C, PUS7, IGF2BP2, IGF2BP1, DNMT3B.

The down-regulated genes were listed from the largest to the smallest of fold changes, and up-regulated genes were listed from the smallest to largest.

ter A (**Figure 4E**). Cluster C subgroup was associated with galactose and glutathione metabolism compared with cluster B (**Figure 4F**), while Cluster C was related to cell cycle pathway; DNA replication and RNA degradation pathway compared with cluster B (**Figure 4G**).

To investigate the potential biological processes and pathways associated with the molecular heterogeneity between cluster A-C, we identified 226 common differential expressed genes between the three clusters in TGCT, which are shown in a Venn diagram (**Figure 4H**). Like RNA modification clusters, GO term analysis revealed that several DEGs enriched in mitochondrial matrix and regulation of cell cycle process (**Figure 4I**). At the same time, several oncological KEGG pathway terms, such as cellular response to decrease oxygen levels and regulation of cell cycle process were enriched in genes (**Figure 4J**). The above analysis highlighted the cellular biological effects related to the identified RNA modification pattern.

Generation and validation of RNA modification prognostic signature

First, complete clinical data, including disease-free survival information, were extracted from 134 of 156 TGCT patients and randomized into training and testing subgroups. Multi-variate cox regression was used to examine the effect of RNA modification regulators on TGCT PFS. The risk stratification score of TGCT was developed with seven selected candidate genes, including TRMT61A, ALKBH1, METTL2B, ALYREF, METTL14, CSTF2 and ADARB1 (**Figure 5A**). The formula for calculating the risk score was as follows:

RNA modification risk signature = 0.295063749328832 * TRMT61A + 0.516321702116629 * ALKBH1 + (-0.579843310502562) * METTL2B + 0.035642951512925 * ALYREF + (-1.04625319354967) * METTL14 + (-0.352420482662729) * CSTF2 + 1.07674658427187 * ADARB1.

Then, we divided TGCT patients in the training cohort into high-risk or low-risk groups according to the medium risk score calculated above as the cut-off point, respectively. Kaplan-Meier survival curves demonstrated that the PFS of the high-risk group with TGCT was better than that of the low-risk group (P<0.001, **Figure 5B**). The distribution of risk scores for patients in the training cohort is shown in **Figure 5B**. The predictive accuracy of the risk score was evaluated by the area under the curve (AUC) of the receiver operator characteristic (ROC) and AUC value of 1-year PFS was 0.911; 2-year was 0.869; 3-year was 0.835; 4-year was 0.881 and 5-year was 0.885 (**Figure 5B**). The above results indicate that the risk score can predict progress-free survival rates in TGCT patients in the training set, which had good validity. Notably, Kaplan-Meier survival analysis in the testing set and entire TGCT set shared similar results with the training set (P = 0.004 for testing set and P<0.001 for entire set, **Figure 5C**, **5D**).

Prognostic performance and clinicopathological relevance

The landscape of corresponding clinicopathological features and the expression level of seven RNA modification risk signature component genes were shown in **Figure 6A**. To further explore the stability and reliability of the risk score as an independent predictor, clinical characteristics and risk score were assessed for the PFS of the patients with TGCT by the univariable and multivariable regression analysis

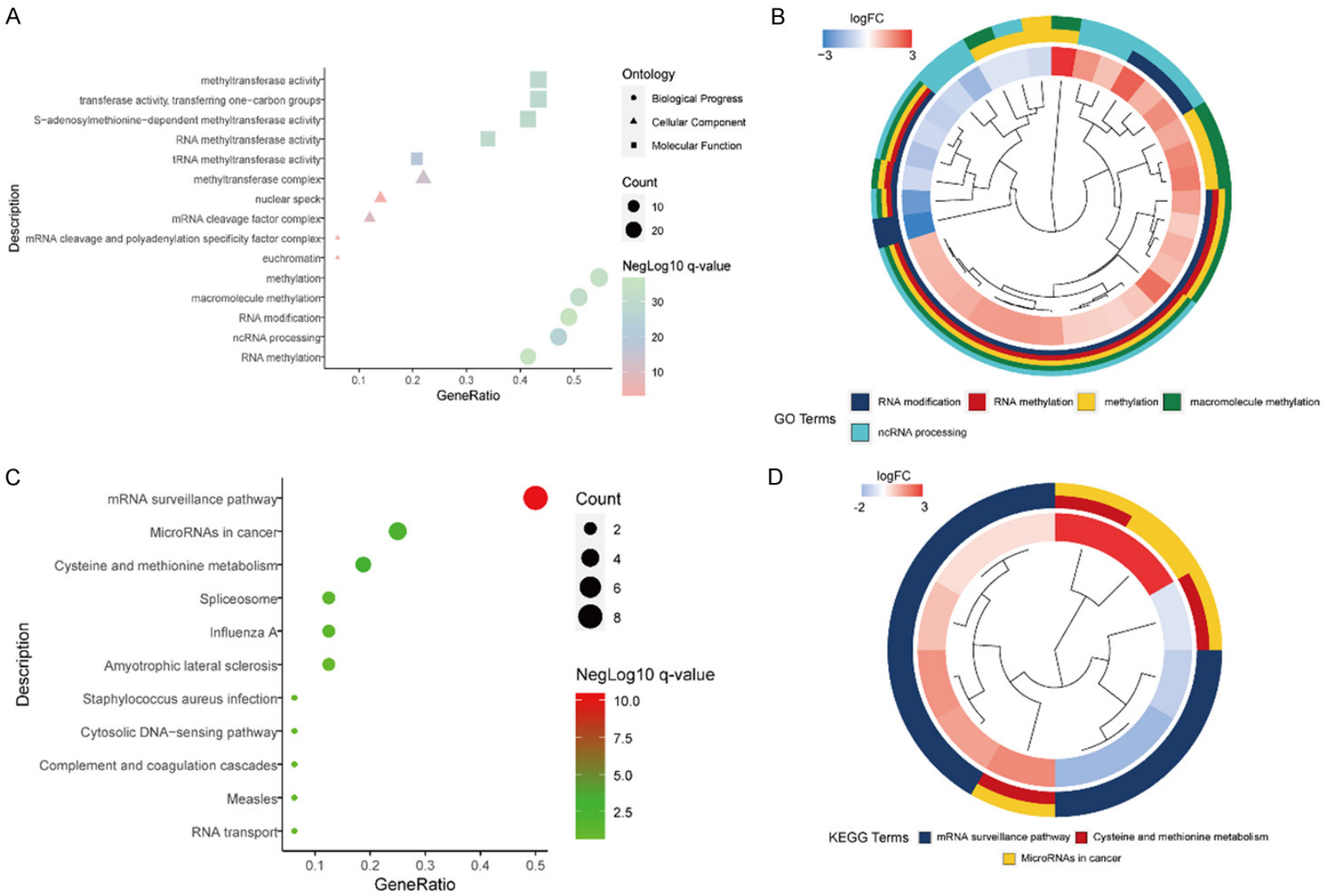

Figure 2. Analysis of RNA modification-related signal pathways. A, B. GO enrichment analysis of 53 RNA modification regulators in TCGA-TGCT cohort. C, D. KEGG pathways analysis of 53 RNA modification regulators.

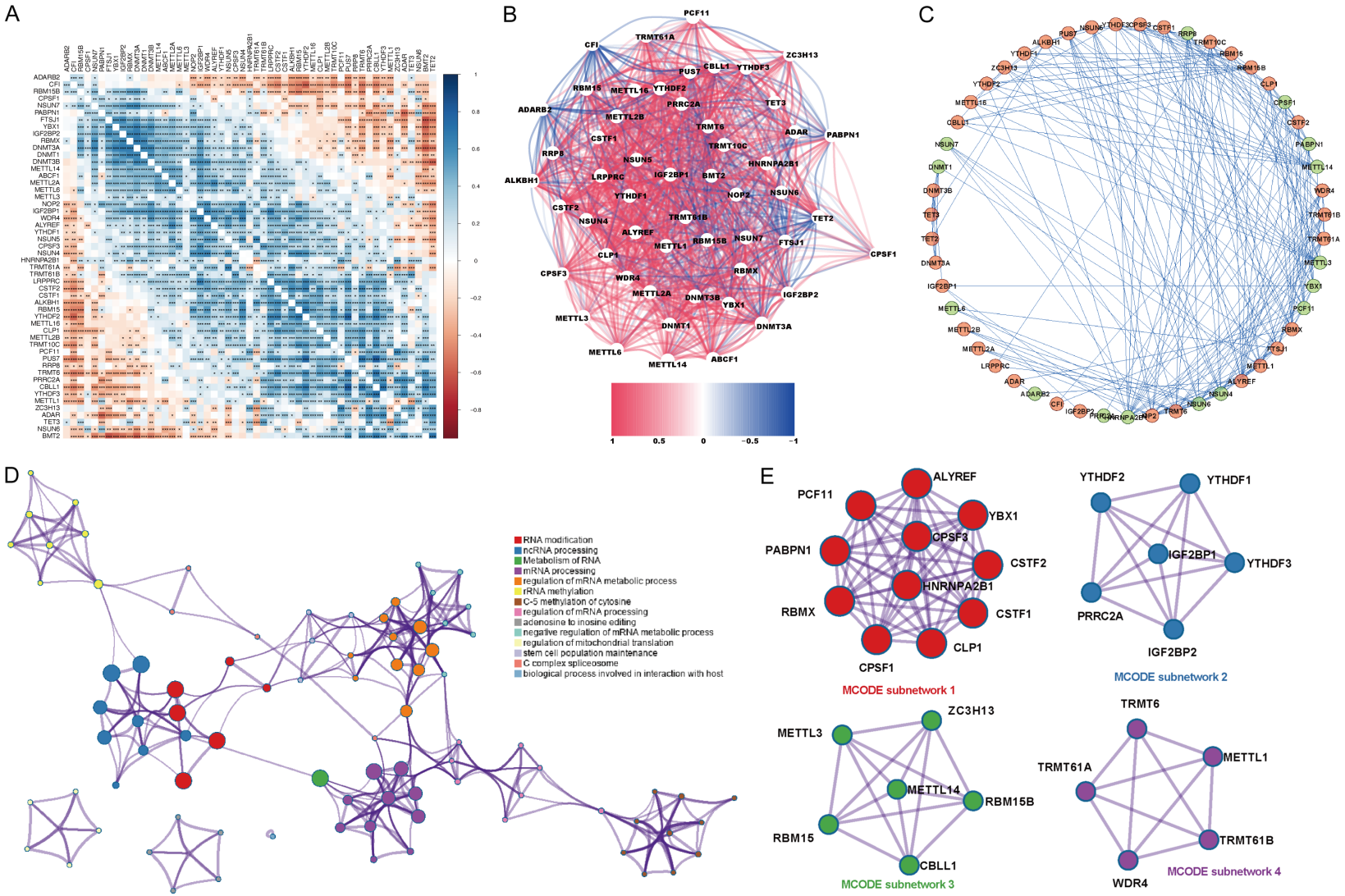

Figure 3. Interaction among RNA modification regulators and functional enrichment. A. Pearson correlation analysis of 53 RNA modification related genes in the TCGA. B. Correlation analysis at the transcriptional level. C. The PPI network showed that correlations with each other. D. The pathway enrichment map of RNA modification regulators downloaded from Metascape software. E. The four highest enrichment sub-modules extracting from plug-in MCODE in Cytoscape.

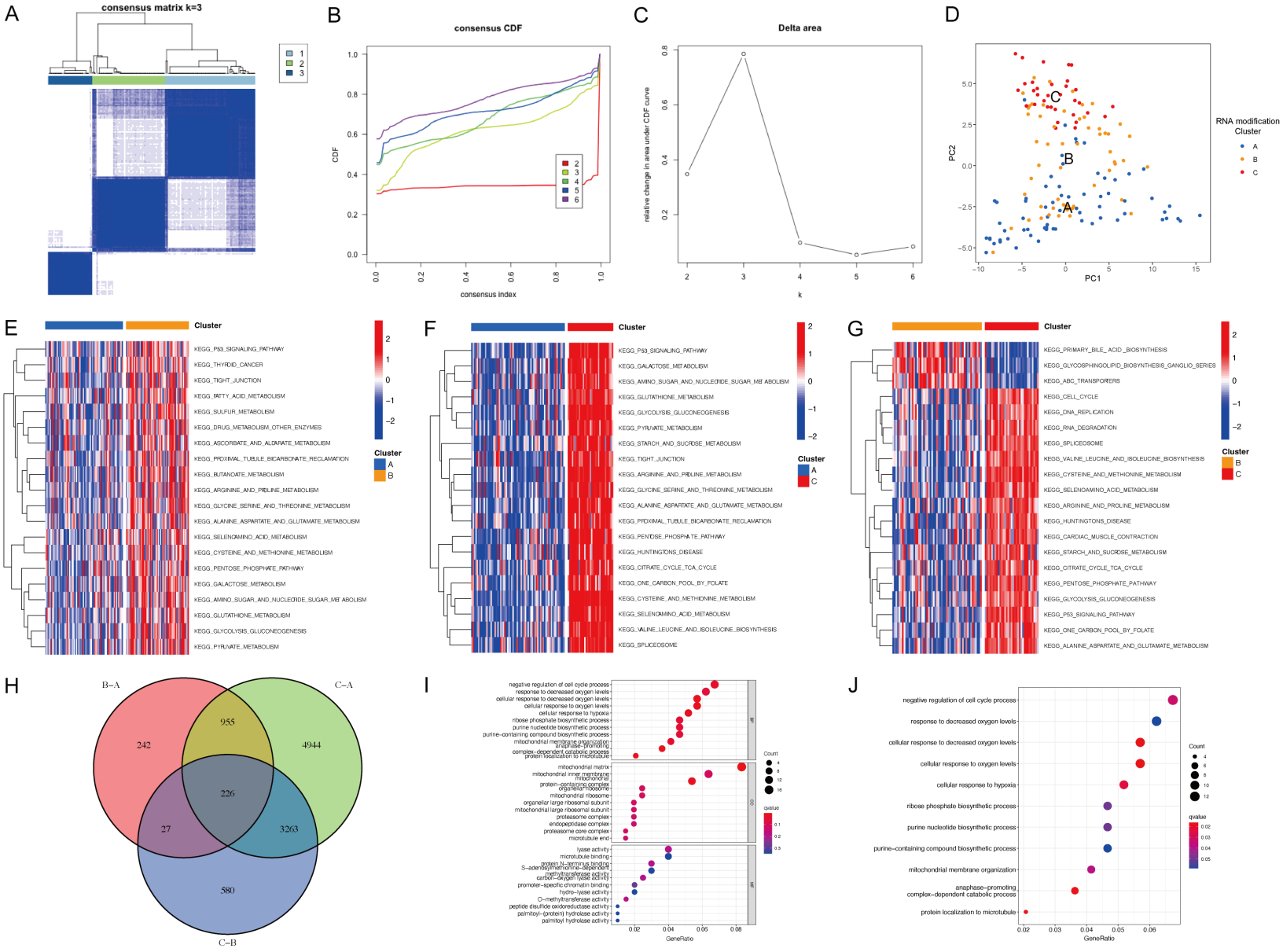
A
consensus matrix k=3
B
consensus CDF
consensus index
CDF
C
Delta area
relative change in area under CDF curve
k
D
RNA modification Cluster
PC1
PC2
E
Cluster
F
Cluster
G
Cluster
H
B–A
C–A
C–B
242
955
4944
226
27
3263
580
I
J
GeneRatio
Count
qvalue

Figure 4. Consensus clustering of RNA modification regulators distinguished three subtypes of TGCT. A. Consensus clustering matrix for the most suitable k = 3. B. Consensus clustering CDF for k = 2 to k = 10. C. Delta area plot showing the relative change in area under the CDF curve from k = 2 to k = 10. D. PCA plot for comparison of the transcriptional profile. E-G. GSVA enrichment analyses of cluster A, B and C. H. The Venn diagram showed that 226 common differential expressed genes between the three clusters in TGCT. I. GO enrichment analysis of 226 DEGs. J. KEGG pathway analysis of 226 DEGs.

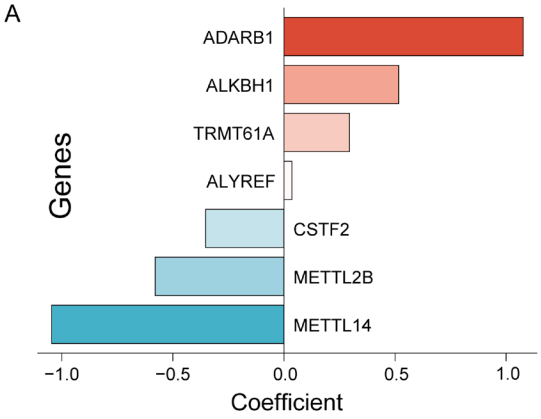

Figure 5. Generation and validation of RNA modification prognostic signature. A. The risk score of TGCT was constructed by selecting seven candidate genes TRMT61A, ALKBH1, METTL2B, ALYREF, METTL14, CSTF2 and ADARB1. B. Kaplan-Meier survival analysis, patient risk score distribution and ROC curve of the training cohort. C. Kaplan-Meier survival analysis, patient risk score distribution and ROC curve of the testing cohort. D. Kaplan-Meier survival analysis, patient risk score distribution and ROC curve of the entire TGCT cohort.

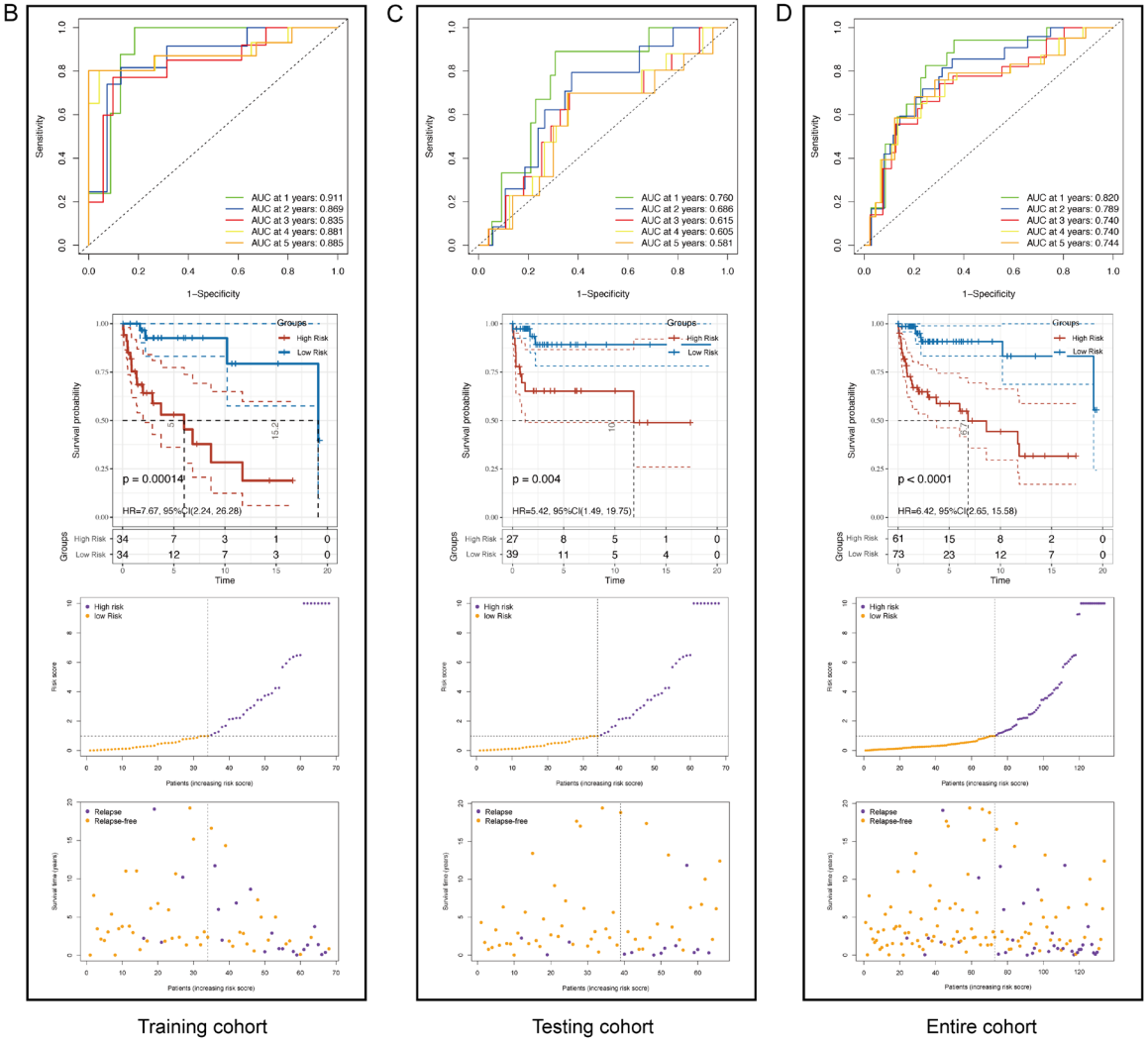

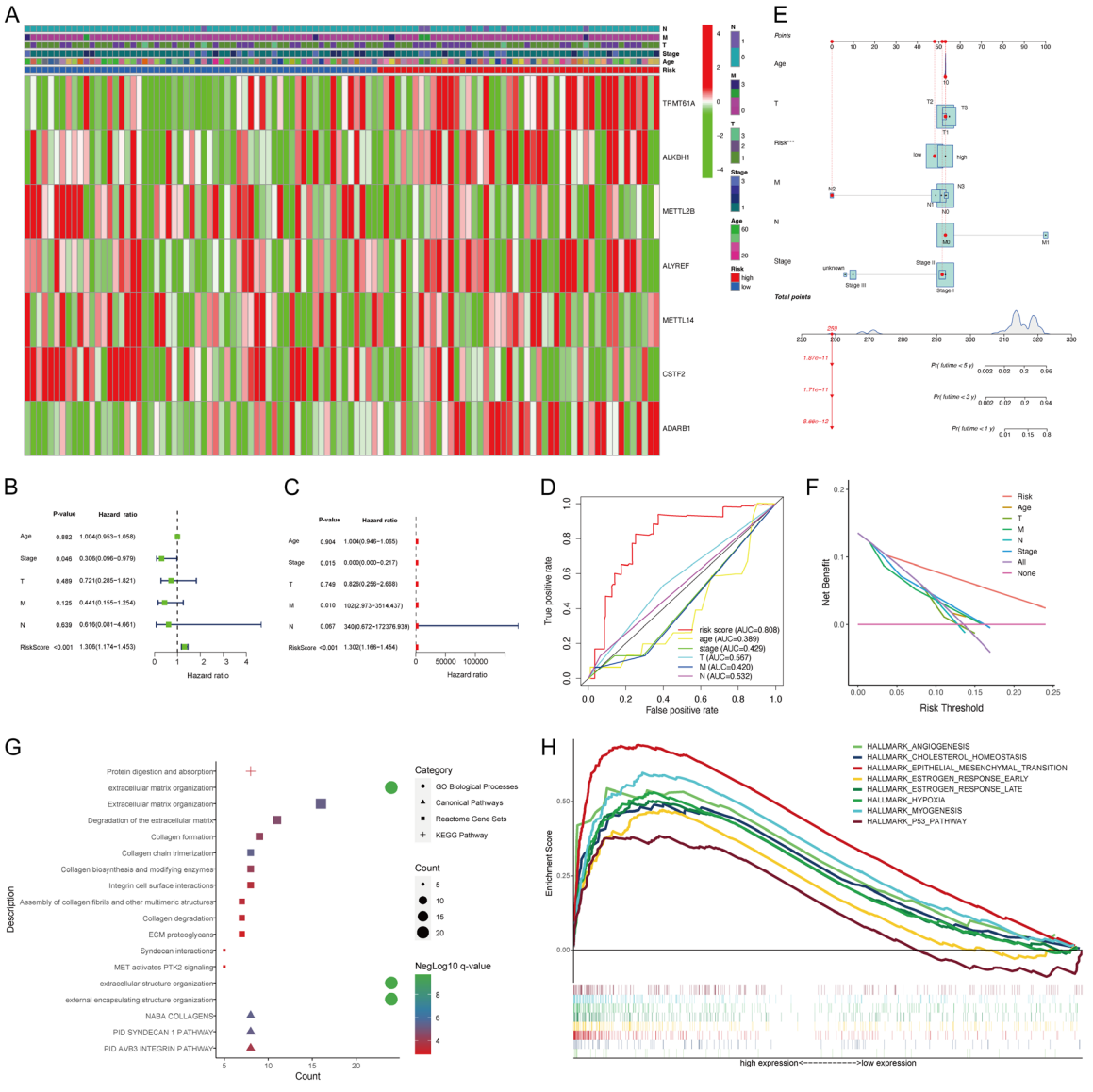

Figure 6. Prognostic performance and clinicopathological relevance. A. A heatmap that revealed the landscape of corresponding clinicopathological features and the expression level of seven genes. B, C. Cox univariate and multivariate analysis of TGCT patients' PFS. D. ROC curve constructed by different clinical variables to evaluate the risk-score as classifiers. E. The nomogram contained seven prognostic factors including stage, T, N, M, age, stage and risk score. F. The curve of comprehensive assessment of prognostic value. G. GO and KEGG functional enrichment analysis of DEGs between high-risk and low-risk groups. H. The eight most significantly enriched signaling pathways from Hallmark GSEA analysis.

in the entire set. In the univariate analysis, the stage (P = 0.046) and this RNA modification signature (P<0.001, HR: 1.036, 95% CI: 1.174 to 1.453) were significantly linked with PFS (**Figure 6B**). The risk score (P<0.001, HR: 1.302, 95% CI: 1.166 to 1.454) were identified by multivariable analysis (**Figure 6C**). Multiple ROC curves were also constructed for various clinical variables, with corresponding AUCs calculated (AUC = 0.808, **Figure 6D**). Additionally, to establish a clinically applicable strategy in TGCT patients, a nomogram was created to evaluate the probability of the 1-year, 3-year, and 5-year PFS. The nomogram was produced by incorporating these 7 independent prognostic predictors, including TNM classification, age, stage, and risk score (**Figure 6E**). After comprehensive assessment of prognostic

value, our results indicated that comparing other clinical characteristics, this risk signature based on RNA modification had superior prognostic accuracy and sustained sensitivity for TGCT patients' PFS (**Figure 6F**).

Functional enrichment of DEGs

To predict the potential function of this developed signature, GO, KEGG and GSEA pathway enrichment analysis, based on differentially expressed genes between high and low-risk groups, were carried out. The signature is enriched in protein digestion and absorption, extracellular matrix organization and epithelial mesenchymal transition (EMT) pathways (**Figure 6G**, **6H**).

Correlation of RNA modification risk signature with tumor microenvironment characteristic

Given the heterogeneity and complexity of the tumor immune microenvironment in TGCT patients, we carried out Cibersoft algorithm to explore the composition of tumor-infiltrating immune cells between high and low-risk groups (**Figure 7A**). NK cells, M2 macrophages and mast cells were significantly enriched in the high-risk group compared to the low-risk group (**Figure 7B**). Furthermore, we calculated immune cell infiltration score by utilizing seven different algorithms, including XCELL [19, 20], TIMER [21, 22], QUANTISEQ [23, 24], MCPCOUNT [25], EPIC [26], CIBERSORT [22, 27] and CIBERSORT-ABS [28]. Spearman correlation analysis between risk score and immune infiltration revealed that high-risk patients tended to harbor higher abundance of hematopoietic stem cell, monocyte and cancer associated fibroblast (**Figure 7C**). Characteristics related to tumor immune microenvironment landscape, including the risk score of different subgroups, are displayed in **Figure 7D**. In addition, we compared several major immune checkpoints gene expression among different subgroups. We found that TNFRSF8, TNFSF9, CD200, CD70, ICOSLG and VTCN1 highly expressed in the high-risk group, while CD244, TNFRSF25, TMIGD2, CD200R1, TNFSF14, CD28, LAG3 and CD160 highly expressed in the low-risk group (**Figure 7E**).

Potential therapeutic strategy for TGCT patients based on risk signature

We compared the response to drugs (IC50) using R package "pRRophetic" for further evaluating the influence of above risk signature for predicting drug therapy response. Among six common TGCT, the drug sensitivity of two showed a significant difference. High-risk patients might be more sensitive to Paclitaxel and Docetaxel, which means patients may benefit from these chemotherapeutic drugs ($P<0.05$, **Figure 8A**). What's more, a CMap database (https://portals.broadinstitute.org/cmap) was conducted to screen out candidate small-molecule drugs [34] showing therapeutic effects on TGCT patients. Then, six small-molecule drugs were finally selected (**Table 3**). The 3D structure tomography of these small-molecule drugs (endo-IWR-1, 2-iminobiotin, BRD-K49367140, emetine, BRD-K95360473 and BRD-K97118047) was found in the PubChem, which could provide possible countermeasures for clinical treatment (**Figure 8B**). Additionally, we applied the GDSC database to explore the predictive sensitivity to anticancer drugs [30]. The results indicated that the most efficient drugs/small molecules were PHA-793887, CP466722, BX-912 and NPK76-II-72-1 (**Figure 8C**).

Experimental verification of seven RNA modification regulators

In order to verify the expression level of seven prognostic RNA modification regulators in TGCT cells, we used qRT-PCR analysis to detect Tcam-2 and Hs 1.Tes cells. Among them, ADARB1, ALYREF and TRMT61A were upregulated in TCGT tumor cells, while ALKBH1, CSTF2, METTL14 and METTL2B were downregulated compared with Hs1Tes normal cells (**Figure 9A**). These findings were basically consistent with the results analyzed in TCGA and GTEx dataset. Here, we chose ADARB1 for further research. In 13 seminoma samples from our institution, the expression level of ADARB1 mRNA was statistically up-regulated in tumor tissues than in normal tissues (**Figure 9B**). Consistent with our PCR results, we observed its tissue abundance using IHC (**Figure 9C**). Additionally, considering epigenetic alterations, such as DNA methylation, which may drive cancer and influence gene expression level, the association between DNA methylation and ADARB1 expression level was explored [35, 36]. We observed four loci of ADARB1 DNA methylation sites which were significantly associated with its expression level in TGCT patients by Spearman correlation analysis, including cg06000635 ($R = 0.420$, $P<0.001$, Figure S2A); cg00927699 ($R = 0.518$, $P<0.001$, Figure

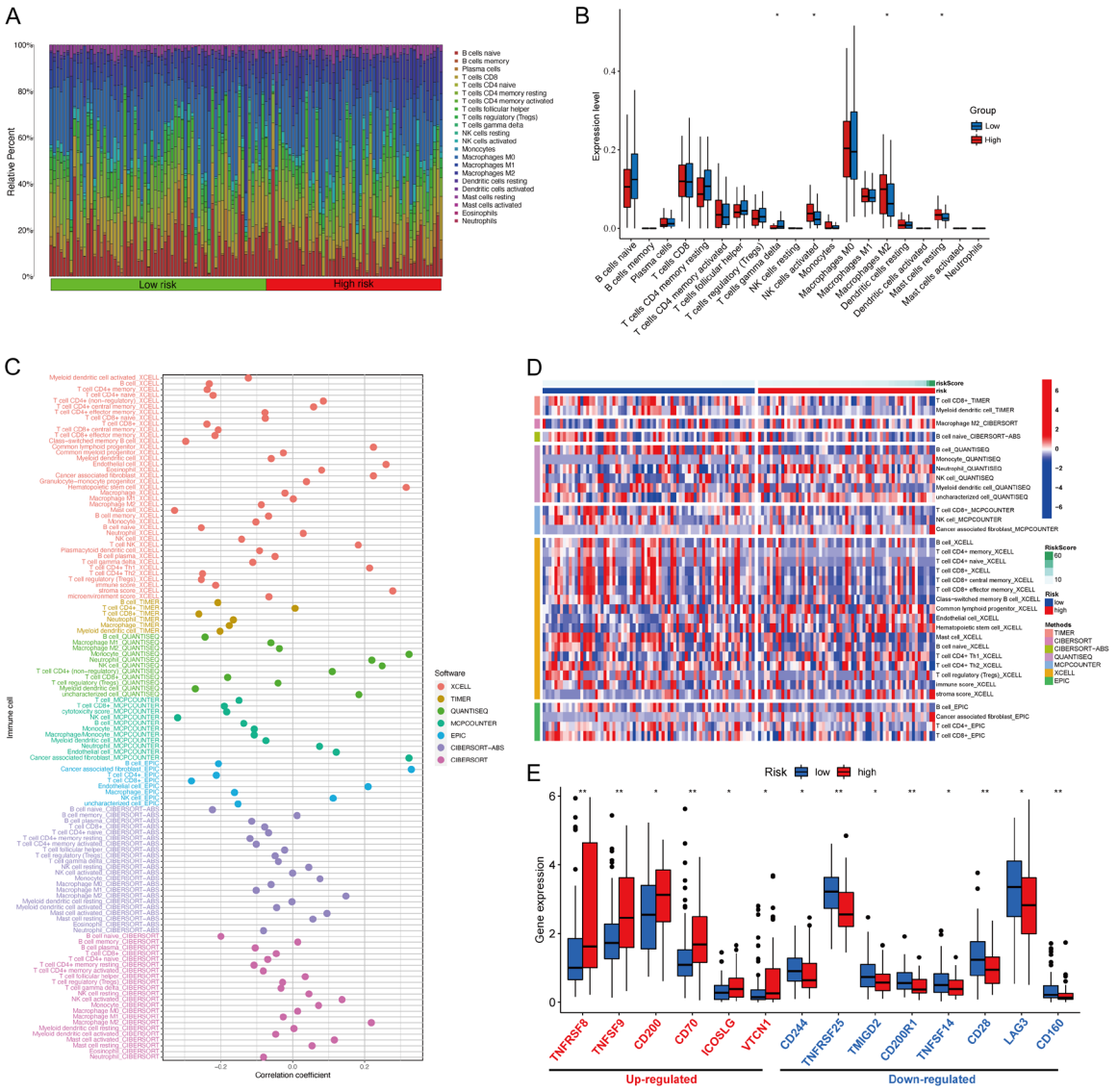

Figure 7. Correlation of RNA modification-risk score with tumor immune-infiltrating characteristic. A. The stacked bar chart indicates the composition of tumor-infiltrating immune cells between high-risk and low-risk groups using Cibersoft algorithm. B. The histogram exhibits the different immune cell fractions between high-risk and low-risk groups. C. Spearman correlation between risk score and immune infiltration. D. Characteristics related to tumor immune microenvironment landscape, including the risk score of different subgroups. E. The histogram that compared several major immune checkpoints gene expression between high-risk group and low-risk group.

S2B); cg09676390 (R = 0.572, *P*<0.001, Figure S2C) and cg27449258 (R = 0.269, *P*<0.001, Figure S2D). Ultimately, we investigated ADARB1 and found that it had a strong positive correlation with NK cells and mast cells. For cytotoxic cells, B cells and T cells, however, there was a negative association with ADARB1 (Figure S2E, S2F). These results suggest that patients with low ADARB1 expression have more possibility to develop an immunosuppressive microenvironment. In conclusion, our study provides new evidence of ADARB1 transcriptional expression and DNA methylation in TGCT patients.

Knockdown ADARB1 suppressed seminoma proliferation and migration

To further investigate the biological function of ADARB1, we generated ADARB1 knockdown Tcam-2 cells with small interfering RNA (siRNA). CCK-8 assays indicated that cell proliferation

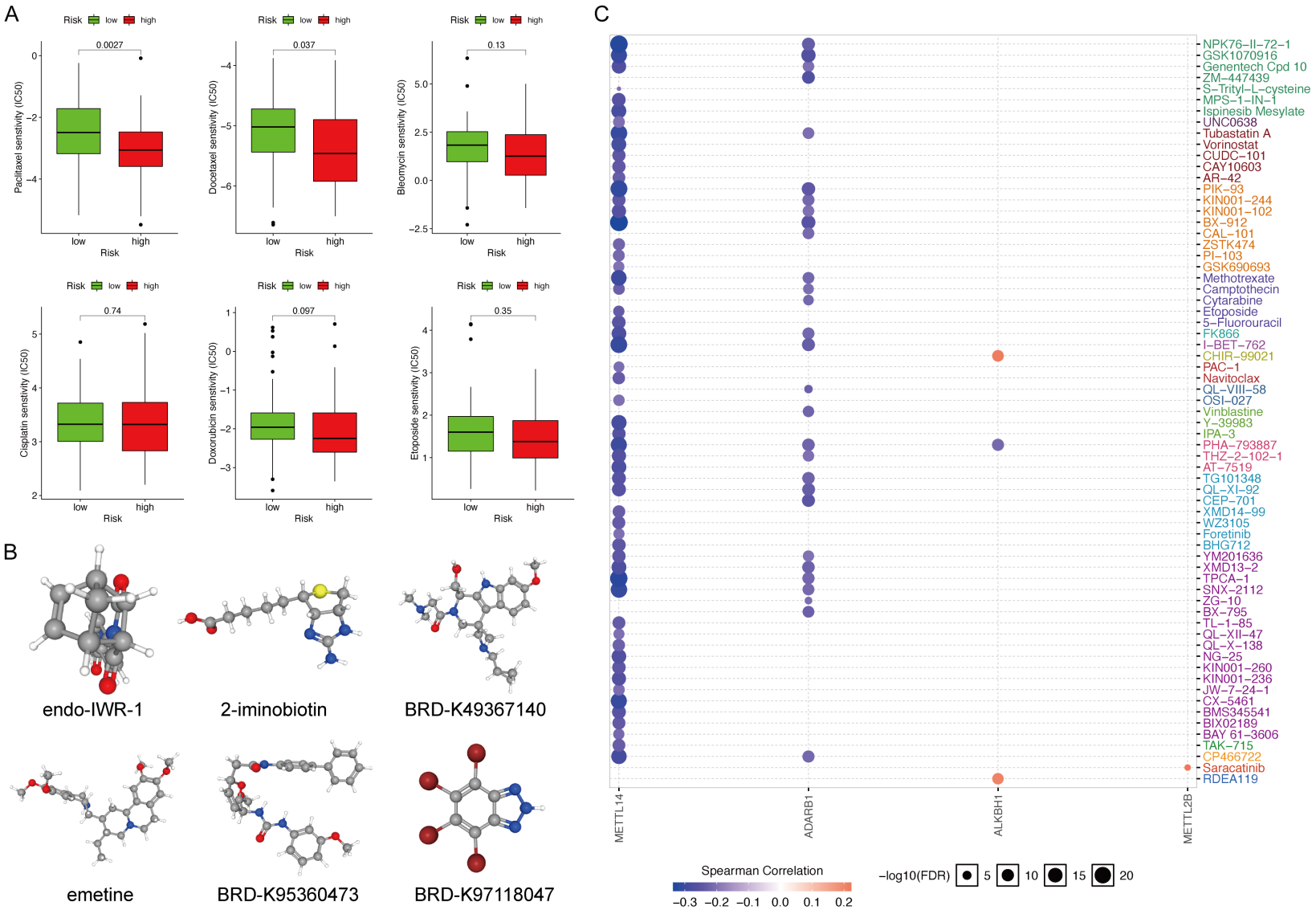

Figure 8. The estimation of chemotherapy response and screened out potential therapeutic strategies for TGCT patients based on risk signature. A. Chemotherapy sensitivity of six common TGCT chemotherapeutic drugs. B. The 3D structure tomography of candidate small-molecule drugs (endo-IWR-1, 2-iminobiotin, BRD-K49367140, emetine, BRD-K95360473 and BRD-K97118047). C. Spearman correlation between the expression status of seven RNA modification regulators and drug sensitivity based on GDSC database.

Table 3. Potential therapeutic small molecular compounds from connectivity map (CMap) website

CMap Name	MoA	-Log10 q-value
endo-IWR-1	PARP inhibitor	15.65
2-iminobiotin	Nitric oxide synthase inhibitor	15.35
BRD-K49367140	/	0.51
emetine	/	0.51
BRD-K95360473	/	0.48
BRD-K97118047	Casein kinase inhibitor	0.45
alizarin	/	0.45
GW-1929	PPAR receptor agonist/Insulin sensitizer	0.42
dilazep	Adenosine receptor antagonist	0.42
alda-1	Aldehyde dehydrogenase activator	0.4

ability was decreased with knockdown of ADARB1 (**Figure 9D**). To determine the long-term impact of ADARB1 on Tcam-2 cell proliferation, Colony formation assay was also performed. We observed lower colony-formation efficiency among knockdown ADARB1 groups than negative control groups after 10 days (**Figure 9E**). Additionally, Transwell migration assay demonstrated that knockdown of ADARB1 could decrease cell metastasis ability remarkably (**Figure 9F**). Collectively, above findings demonstrated that ADARB1 may act as a positive regulator of tumor proliferation and migration among seminoma patients.

Discussion

Testicular germ cell tumor (TGCT) is the most common subtype of testicular cancers, heavily affecting the reproductive health of young men [37]. TGCT accounts for about 1% of male cancers. In recent years, the incidence of TGCT has increased rapidly worldwide, especially among Caucasian populations [38]. TGCT is highly sensitive to conventional chemotherapy and considered as a kind of highly curable cancer. However, the inevitable toxicity of chemotherapy might cause damage to other organs of the patient and affect long-term survival [37, 39]. A total of 10-20% of TCGT patients cannot be cured by conventional chemotherapy [40]. As a result, it requires great priority to identify essential biomarkers that can improve chemotherapy sensitivity, overcome cancer drug resistance and improve patient's outcomes.

Emerging evidence has proven that the dysregulation of RNA modification has become a critical posttranscriptional regulator of gene expression, which could have therapeutic potential in the future [9, 41]. N6-methyladenosine (m6A) has been shown to be related to the occurrence and progression of multiple tumors, including glioblastoma (GBM), acute myeloid leukemia (AML) and acute myeloid leukemia (AML) [42]. Interestingly, m6A often acts as a double-edged sword in different tumor types. Low m6A level on ADAM19 enhances its expression, promotes GSCs growth and finally leads to tumorigenesis [43]. Conversely, the enhanced m6A modification of SOCS2 promotes its degradation, which accelerates tumor progression in HCC [44]. This indicates that the methylation modification is a complex process, involving many methylation regulating factors. Different methylation regulators interact with each other to perform biological functions.

In this study, we classified seven major types of RNA modifications and 75 corresponding RNA regulatory factors. Firstly, we identified genes related to RNA modifications that are differentially expressed in testicular cancer and normal tissues. The results showed that most RNA modification regulators such as NSUN5 and IGF2BPs were abnormally expressed in TGCT. Recent studies reported that epigenetic loss of RNA-methyltransferase NSUN5 in glioma is significantly related with long-term survival of glioma patients [45]. Another study found that m6A reader IGF2BPs proteins drive RCC tumorigenesis and metastasis via enhancing S1PR3 mRNA stabilization [46]. This further illustrated that these RNA modification regulators may be involved in the development and prognosis of testicular germ cell tumors. Performing KEGG and GO enrichment analysis, we explored the biological function involved in differentially expressed RNA modification regulatory factors. DEGs are mainly concentrated on mRNA surveillance pathways, microRNA in cancer and cysteine/methionine metabolism. The mRNA surveillance mechanisms is aimed at checking the fidelity at each step of mRNA manufacture [47]. Incorrect activation and inactivation of these enriched pathways often lead to tumors. Next, through multivariate Cox regression, we established a prognostic risk signature consist-

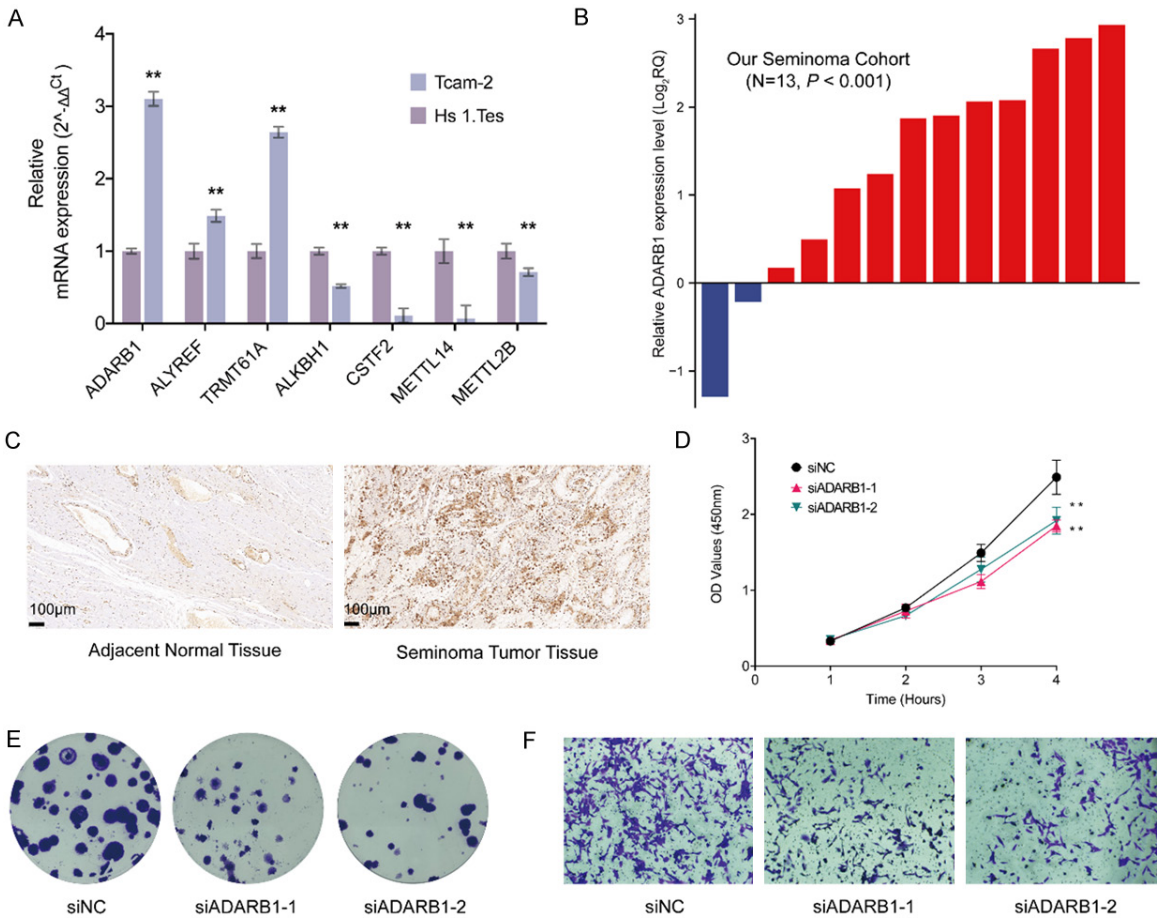

Figure 9. Experimental verification of seven RNA modification regulators. A. qRT-PCR analysis to verify the expression level of seven prognostic RNA modification regulators in TGCT cells. B. The expression level of ADARB1 among 13 seminoma patients in our cohort. C. IHC revealed upregulated expression of ADARB1 in seminoma patients. D. CCK-8 assay demonstrated knockdown ADARB1 could inhibit Tcam-2 cells proliferation. E. Colony formation assay of knockdown ADARB1. F. Transwell migration assay for evaluating the migration ability of Tcam-2 cells after silencing ADARB1.

ing of 7 RNA modification regulatory factors. TRMT61A, ALKBH1, ALYREF, and ADARB1 were positively related to risk score while CSTF2, METTL14 and METTL2B showed contrast correlation. As it is known, TRMT61A acts as a methylation modification regulator that can methylate tRNA, loss of which increased death of glioma cells [48]. ALYREF can bind to m5C sites in 3'-untranslated (3'-UTR) regions of PKM2 mRNA and promote bladder cancer cell proliferation by PKM2-mediated glycolysis [49]. Interestingly, it has been reported that CSTF2 regulated the tumorigenic functions in UCB cells, and enhanced tumor proliferation, migration, and invasion [50]. However, our study demonstrated CSTF2 as a negative factor of risk score and functioned as a protector in inhibiting tumorigenesis. In conclusion, RNA modification regulators may play tumor-specific roles in different neoplastic process.

Based on these seven genes, we divided 134 TCGT patients into three clusters by Consensus clustering. To figure out different characteristics between groups, we further compared the differences in pathways among each cluster using GSVA analysis. These differential pathways were involved in the distinct progression of the three RNA modification-related subtypes of TGCT. Some significant differential pathways could be activated in different TGCT RNA modification clusters, such as the p53 signaling pathway and glucometabolic pathway. P53, is a classical tumor suppressor gene and mutant p53 proteins can exert oncogenic functions [51, 52]. Under low energy supply, glycolysis is

the primary way to producd energy for maintaining cancer cell proliferation, which is conducive to tumor invasion [52, 53]. Patients of cluster C may benefit more from drugs targeting these signaling pathways, rather than from glycosphingolipid biosynthesis pathways.

Furthermore, testicular germ cell tumors can be characterized as immunological tumors with large numbers of immune cell infiltrated during routine pathological evaluation of biopsy samples from TGCT patients [54-56]. In our study, we separately analyzed the tumor microenvironment of immune infiltrating cells, and compared the difference and correlation between the high- low-risk groups. Notably, the establishment of predictive biomarkers for checkpoint immunotherapy was of great significant of maximizing therapeutic benefit [57]. Here, we have elucidated the expression of immune checkpoints between TGCT patients and healthy population, which may be helpful for the personalized cancer immunotherapy. We compared the response to drugs by calculating the IC50 value and screened out candidate small-molecule compounds which may provide possible solutions for clinical treatment. Ultimately, we further confirmed ADARB1 was significantly up-regulated in seminoma patients both in mRNA and protein level. Lu et al. has reported that aberrant expression of ADARB1 facilitates Temozolomide chemoresistance and immune infiltration in glioblastoma [58]. Nevertheless, the biological function of ADARB1 in TGCT patients remains to be discovered. Here, we revealed ADARB1 serves as a promising targetable biomarker for seminoma progression and provides a potential therapeutic application for clinical treatment.

Conclusion

We comprehensively analyzed the expression of various RNA modification regulators in TGCT. They showed not only great value for prognosis prediction but are also closely associated with tumor immune microenvironment and immunotherapy. The sensitivity of chemotherapy drugs and candidate small molecular compounds were finally identified, which could better guide clinical medication. We hope the findings of this study may contribute to further investigation of the mechanism of these RNA modification regulators and acquire more clinical benefit in TGCT patients.

Disclosure of conflict of interest

None.

Address correspondence to: Shilei Qian, Department of Urology, Binhai People's Hospital, Yancheng 224500, Jiangsu, China. E-mail: qslmnwk123@163.com

References

[1] Batool A, Karimi N, Wu XN, Chen SR and Liu YX. Testicular germ cell tumor: a comprehensive review. Cell Mol Life Sci 2019; 76: 1713-1727.

[2] Siska PJ, Johnpulle RAN, Zhou A, Bordeaux J, Kim JY, Dabbas B, Dakappagari N, Rathmell JC, Rathmell WK, Morgans AK, Balko JM and Johnson DB. Deep exploration of the immune infiltrate and outcome prediction in testicular cancer by quantitative multiplexed immunohistochemistry and gene expression profiling. Oncoimmunology 2017; 6: e1305535.

[3] Winter C and Albers P. Testicular germ cell tumors: pathogenesis, diagnosis and treatment. Nat Rev Endocrinol 2011; 7: 43-53.

[4] Lobo J, Costa AL, Vilela-Salgueiro B, Rodrigues Â, Guimarães R, Cantante M, Lopes P, Antunes L, Jerónimo C and Henrique R. Testicular germ cell tumors: revisiting a series in light of the new WHO classification and AJCC staging systems, focusing on challenges for pathologists. Hum Pathol 2018; 82: 113-124.

[5] Rajpert-De Meyts E, McGlynn KA, Okamoto K, Jewett MA and Bokemeyer C. Testicular germ cell tumours. Lancet 2016; 387: 1762-1774.

[6] Honecker F, Aparicio J, Berney D, Beyer J, Bokemeyer C, Cathomas R, Clarke N, Cohn-Cedermark G, Daugaard G, Dieckmann KP, Fizazi K, Fossa S, Germa-Lluch JR, Giannatempo P, Gietema JA, Gillessen S, Haugnes HS, Heidenreich A, Hemminki K, Huddart R, Jewett MAS, Joly F, Lauritsen J, Lorch A, Necchi A, Nicolai N, Oing C, Oldenburg J, Ondrus D, Papachristofilou A, Powles T, Sohaib A, Stahl O, Tandstad T, Toner G and Horwich A. ESMO consensus conference on testicular germ cell cancer: diagnosis, treatment and follow-up. Ann Oncol 2018; 29: 1658-1686.

[7] Albers P, Albrecht W, Algaba F, Bokemeyer C, Cohn-Cedermark G, Fizazi K, Horwich A and Laguna MP; European Association of Urology. EAU guidelines on testicular cancer: 2011 update. Eur Urol 2011; 60: 304-319.

[8] Azak A, Oksuzoglu B, Deren T, Onec BM and Zengin N. Cerebrovascular accident during cisplatin-based combination chemotherapy of testicular germ cell tumor: an unusual case report. Anticancer Drugs 2008; 19: 97-98.

[9] Barbieri I and Kouzarides T. Role of RNA modifications in cancer. Nat Rev Cancer 2020; 20: 303-322.

[10] Jonkhout N, Tran J, Smith MA, Schonrock N, Mattick JS and Novoa EM. The RNA modification landscape in human disease. RNA 2017; 23: 1754-1769.
[11] Yao RW, Wang Y and Chen LL. Cellular functions of long noncoding RNAs. Nat Cell Biol 2019; 21: 542-551.
[12] Gebert LFR and MacRae IJ. Regulation of microRNA function in animals. Nat Rev Mol Cell Biol 2019; 20: 21-37.
[13] Delaunay S and Frye M. RNA modifications regulating cell fate in cancer. Nat Cell Biol 2019; 21: 552-559.
[14] Lee SA, Lee KH, Kim H and Cho JY. METTL8 mRNA methyltransferase enhances cancer cell migration via direct binding to ARID1A. Int J Mol Sci 2021; 22: 5432.
[15] Yang Y, Hsu PJ, Chen YS and Yang YG. Dynamic transcriptomic m(6)A decoration: writers, erasers, readers and functions in RNA metabolism. Cell Res 2018; 28: 616-624.
[16] Shi H, Chai P, Jia R and Fan X. Novel insight into the regulatory roles of diverse RNA modifications: re-defining the bridge between transcription and translation. Mol Cancer 2020; 19: 78.
[17] Bohnsack KE, Hobartner C and Bohnsack MT. Eukaryotic 5-methylcytosine (m(5)C) RNA methyltransferases: mechanisms, cellular functions, and links to disease. Genes (Basel) 2019; 10: 102.
[18] Miranda-Gonçalves V, Lobo J, Guimarães-Teixeira C, Barros-Silva D, Guimarães R, Cantante M, Braga I, Maurício J, Oing C, Honecker F, Nettersheim D, Looijenga LHJ, Henrique R and Jerónimo C. The component of the mA writer complex VIRMA is implicated in aggressive tumor phenotype, DNA damage response and cisplatin resistance in germ cell tumors. J Exp Clin Cancer Res 2021; 40: 268.
[19] Aran D. Cell-type enrichment analysis of bulk transcriptomes using xCell. Methods Mol Biol 2020; 2120: 263-276.
[20] Aran D, Hu Z and Butte AJ. xCell: digitally portraying the tissue cellular heterogeneity landscape. Genome Biol 2017; 18: 220.
[21] Li T, Fu J, Zeng Z, Cohen D, Li J, Chen Q, Li B and Liu XS. TIMER2.0 for analysis of tumor-infiltrating immune cells. Nucleic Acids Res 2020; 48: W509-W514.
[22] Chen B, Khodadoust MS, Liu CL, Newman AM and Alizadeh AA. Profiling tumor infiltrating immune cells with CIBERSORT. Methods Mol Biol 2018; 1711: 243-259.
[23] Finotello F, Mayer C, Plattner C, Laschober G, Rieder D, Hackl H, Krogsdam A, Loncova Z, Posch W, Wilflingseder D, Sopper S, Ijsselsteijn M, Brouwer TP, Johnson D, Xu Y, Wang Y, Sanders ME, Estrada MV, Ericsson-Gonzalez P, Charoentong P, Balko J, de Miranda NFDCC and Trajanoski Z. Molecular and pharmacological modulators of the tumor immune contexture revealed by deconvolution of RNA-seq data. Genome Med 2019; 11: 34.
[24] Plattner C, Finotello F and Rieder D. Deconvoluting tumor-infiltrating immune cells from RNA-seq data using quanTIseq. Methods Enzymol 2020; 636: 261-285.
[25] Dienstmann R, Villacampa G, Sveen A, Mason MJ, Niedzwiecki D, Nesbakken A, Moreno V, Warren RS, Lothe RA and Guinney J. Relative contribution of clinicopathological variables, genomic markers, transcriptomic subtyping and microenvironment features for outcome prediction in stage II/III colorectal cancer. Ann Oncol 2019; 30: 1622-1629.
[26] Racle J, de Jonge K, Baumgaertner P, Speiser DE and Gfeller D. Simultaneous enumeration of cancer and immune cell types from bulk tumor gene expression data. Elife 2017; 6: e26476.
[27] Zhang H, Li R, Cao Y, Gu Y, Lin C, Liu X, Lv K, He X, Fang H, Jin K, Fei Y, Chen Y, Wang J, Liu H, Li H, Zhang H, He H and Zhang W. Poor clinical outcomes and immunoevasive contexture in intratumoral IL-10-producing macrophages enriched gastric cancer patients. Ann Surg 2022; 275: e626-e635.
[28] Tamminga M, Hiltermann TJN, Schuuring E, Timens W, Fehrmann RS and Groen HJ. Immune microenvironment composition in non-small cell lung cancer and its association with survival. Clin Transl Immunology 2020; 9: e1142.
[29] Auslander N, Zhang G, Lee JS, Frederick DT, Miao B, Moll T, Tian T, Wei Z, Madan S, Sullivan RJ, Boland G, Flaherty K, Herlyn M and Ruppin E. Robust prediction of response to immune checkpoint blockade therapy in metastatic melanoma. Nat Med 2018; 24: 1545-1549.
[30] Yang W, Soares J, Greninger P, Edelman EJ, Lightfoot H, Forbes S, Bindal N, Beare D, Smith JA, Thompson IR, Ramaswamy S, Futreal PA, Haber DA, Stratton MR, Benes C, McDermott U and Garnett MJ. Genomics of Drug Sensitivity in Cancer (GDSC): a resource for therapeutic biomarker discovery in cancer cells. Nucleic Acids Res 2013; 41: D955-D961.
[31] Chen H, Yao J, Bao R, Dong Y, Zhang T, Du Y, Wang G, Ni D, Xun Z, Niu X, Ye Y and Li HB. Cross-talk of four types of RNA modification writers defines tumor microenvironment and pharmacogenomic landscape in colorectal cancer. Mol Cancer 2021; 20: 29.
[32] Cerami E, Gao J, Dogrusoz U, Gross BE, Sumer SO, Aksoy BA, Jacobsen A, Byrne CJ, Heuer ML, Larsson E, Antipin Y, Reva B, Goldberg AP, Sander C and Schultz N. The cBio cancer genomics portal: an open platform for exploring

multidimensional cancer genomics data. Cancer Discov 2012; 2: 401-404.
[33] Li T, Fan J, Wang B, Traugh N, Chen Q, Liu JS, Li B and Liu XS. TIMER: a web server for comprehensive analysis of tumor-infiltrating immune cells. Cancer Res 2017; 77: e108-e110.
[34] Lamb J, Crawford ED, Peck D, Modell JW, Blat IC, Wrobel MJ, Lerner J, Brunet JP, Subramanian A, Ross KN, Reich M, Hieronymus H, Wei G, Armstrong SA, Haggarty SJ, Clemons PA, Wei R, Carr SA, Lander ES and Golub TR. The connectivity map: using gene-expression signatures to connect small molecules, genes, and disease. Science 2006; 313: 1929-1935.
[35] Pan H, Renaud L, Chaligne R, Bloehdorn J, Tausch E, Mertens D, Fink AM, Fischer K, Zhang C, Betel D, Gnirke A, Imielinski M, Moreaux J, Hallek M, Meissner A, Stilgenbauer S, Wu CJ, Elemento O and Landau DA. Discovery of candidate DNA methylation cancer driver genes. Cancer Discov 2021; 11: 2266-2281.
[36] Li D, Zhao W, Zhang X, Lv H, Li C and Sun L. NEFM DNA methylation correlates with immune infiltration and survival in breast cancer. Clin Epigenetics 2021; 13: 112.
[37] Fung C, Dinh PC, Fossa SD and Travis LB. Testicular cancer survivorship. J Natl Compr Canc Netw 2019; 17: 1557-1568.
[38] Znaor A, Lortet-Tieulent J, Jemal A and Bray F. International variations and trends in testicular cancer incidence and mortality. Eur Urol 2014; 65: 1095-1106.
[39] Chovanec M, Hanna N, Cary KC, Einhorn L and Albany C. Management of stage I testicular germ cell tumours. Nat Rev Urol 2016; 13: 663-673.
[40] de Vries G, Rosas-Plaza X, van Vugt MATM, Gietema JA and de Jong S. Testicular cancer: determinants of cisplatin sensitivity and novel therapeutic opportunities. Cancer Treat Rev 2020; 88: 102054.
[41] Nombela P, Miguel-López B and Blanco S. The role of mA, mC and Ψ RNA modifications in cancer: novel therapeutic opportunities. Mol Cancer 2021; 20: 18.
[42] Sun T, Wu R and Ming L. The role of m6A RNA methylation in cancer. Biomed Pharmacother 2019; 112: 108613.
[43] Cui Q, Shi H, Ye P, Li L, Qu Q, Sun G, Sun G, Lu Z, Huang Y, Yang CG, Riggs AD, He C and Shi Y. m6A RNA methylation regulates the self-renewal and tumorigenesis of glioblastoma stem cells. Cell Rep 2017; 18: 2622-2634.
[44] Chen M, Wei L, Law CT, Tsang FH, Shen J, Cheng CL, Tsang LH, Ho DW, Chiu DK, Lee JM, Wong CC, Ng IO and Wong CM. RNA N6-methyladenosine methyltransferase-like 3 promotes liver cancer progression through YTHDF2-dependent posttranscriptional silencing of SOCS2. Hepatology 2018; 67: 2254-2270.
[45] Janin M, Ortiz-Barahona V, de Moura MC, Martínez-Cardús A, Llinàs-Arias P, Soler M, Nachmani D, Pelletier J, Schumann U, Calleja-Cervantes ME, Moran S, Guil S, Bueno-Costa A, Piñeyro D, Perez-Salvia M, Rosselló-Tortella M, Piqué L, Bech-Serra JJ, De La Torre C, Vidal A, Martínez-Iniesta M, Martín-Tejera JF, Villanueva A, Arias A, Cuartas I, Aransay AM, La Madrid AM, Carcaboso AM, Santa-Maria V, Mora J, Fernandez AF, Fraga MF, Aldecoa I, Pedrosa L, Graus F, Vidal N, Martínez-Soler F, Tortosa A, Carrato C, Balañá C, Boudreau MW, Hergenrother PJ, Kötter P, Entian KD, Hench J, Frank S, Mansouri S, Zadeh G, Dans PD, Orozco M, Thomas G, Blanco S, Seoane J, Preiss T, Pandolfi PP and Esteller M. Epigenetic loss of RNA-methyltransferase NSUN5 in glioma targets ribosomes to drive a stress adaptive translational program. Acta Neuropathol 2019; 138: 1053-1074.
[46] Ying Y, Ma X, Fang J, Chen S, Wang W, Li J, Xie H, Wu J, Xie B, Liu B, Wang X, Zheng X and Xie L. EGR2-mediated regulation of mA reader IGF2BP proteins drive RCC tumorigenesis and metastasis via enhancing S1PR3 mRNA stabilization. Cell Death Dis 2021; 12: 750.
[47] Vasudevan S, Peltz SW and Wilusz CJ. Non-stop decay–a new mRNA surveillance pathway. Bioessays 2002; 24: 785-788.
[48] Macari F, El-Houfi Y, Boldina G, Xu H, Khoury-Hanna S, Ollier J, Yazdani L, Zheng G, Bièche I, Legrand N, Paulet D, Durrieu S, Byström A, Delbecq S, Lapeyre B, Bauchet L, Pannequin J, Hollande F, Pan T, Teichmann M, Vagner S, David A, Choquet A and Joubert D. TRM6/61 connects PKCα with translational control through tRNAi(Met) stabilization: impact on tumorigenesis. Oncogene 2016; 35: 1785-1796.
[49] Wang JZ, Zhu W, Han J, Yang X, Zhou R, Lu HC, Yu H, Yuan WB, Li PC, Tao J, Lu Q, Wei JF and Yang H. The role of the HIF-1α/ALYREF/PKM2 axis in glycolysis and tumorigenesis of bladder cancer. Cancer Commun (Lond) 2021; 41: 560-575.
[50] Chen X, Zhang JX, Luo JH, Wu S, Yuan GJ, Ma NF, Feng Y, Cai MY, Chen RX, Lu J, Jiang LJ, Chen JW, Jin XH, Liu HL, Chen W, Guan XY, Kang TB, Zhou FJ and Xie D. CSTF2-induced shortening of the 3'UTR promotes the pathogenesis of urothelial carcinoma of the bladder. Cancer Res 2018; 78: 5848-5862.
[51] Muller PA and Vousden KH. p53 mutations in cancer. Nat Cell Biol 2013; 15: 2-8.
[52] Ganapathy-Kanniappan S and Geschwind JF. Tumor glycolysis as a target for cancer therapy: progress and prospects. Mol Cancer 2013; 12: 152.

[53] Cao L, Wu J, Qu X, Sheng J, Cui M, Liu S, Huang X, Xiang Y, Li B, Zhang X and Cui R. Glycometabolic rearrangements--aerobic glycolysis in pancreatic cancer: causes, characteristics and clinical applications. J Exp Clin Cancer Res 2020; 39: 267.

[54] Klein B, Schuppe HC, Bergmann M, Hedger MP, Loveland BE and Loveland KL. An in vitro model demonstrates the potential of neoplastic human germ cells to influence the tumour microenvironment. Andrology 2017; 5: 763-770.

[55] Klein B, Haggeney T, Fietz D, Indumathy S, Loveland KL, Hedger M, Kliesch S, Weidner W, Bergmann M and Schuppe HC. Specific immune cell and cytokine characteristics of human testicular germ cell neoplasia. Hum Reprod 2016; 31: 2192-2202.

[56] Hvarness T, Nielsen JE, Almstrup K, Skakkebaek NE, Rajpert-De Meyts E and Claesson MH. Phenotypic characterisation of immune cell infiltrates in testicular germ cell neoplasia. J Reprod Immunol 2013; 100: 135-145.

[57] Yang Y. Cancer immunotherapy: harnessing the immune system to battle cancer. J Clin Invest 2015; 125: 3335-3337.

[58] Lu C, Chen X, Yan Y, Ren X, Wang X, Peng B, Cai Y, Liang Q, Xu Z and Peng J. Aberrant expression of ADARB1 facilitates temozolomide chemoresistance and immune infiltration in glioblastoma. Front Pharmacol 2022; 13: 768743.

Table S1. Oligonucleotide sequences used in the present study

Primers	Sequences	
TRMT61A	Forward	AGCTTCGTGGCATACGAGG
	Reverse	CCGATAAGGTCAACTGAGTGC
METTL2B	Forward	ACCGAATACTGGAGGTTGGC
	Reverse	ACAGGTCGTGAACAAAGGCA
METTL14	Forward	AGTGCCGACAGCATTGGTG
	Reverse	GGAGCAGAGGTATCATAGGAAGC
CSTF2	Forward	CAGCGGTGGATCGTTCTCTAC
	Reverse	AACAACAGGTCCAACCTCAGA
ALYREF	Forward	GCAGGCCAAAACAACTTCCC
	Reverse	AGTTCCTGAATATCGGCGTCT
ALKBH1	Forward	AAACTTTTCCGCTTCTACCGTC
	Reverse	TTTGAGTCCATAGGCTTGCCA
ADARB1	Forward	GTGAAGGAAAACCGCAATCTGG
	Reverse	CAGGAGTGTGTACTGCAAACC
β-actin	Forward	ATGACTTAGTTGCGTTACACC
	Reverse	GACTTCCTGTAACAACGCATC

RNA modification in TGCT

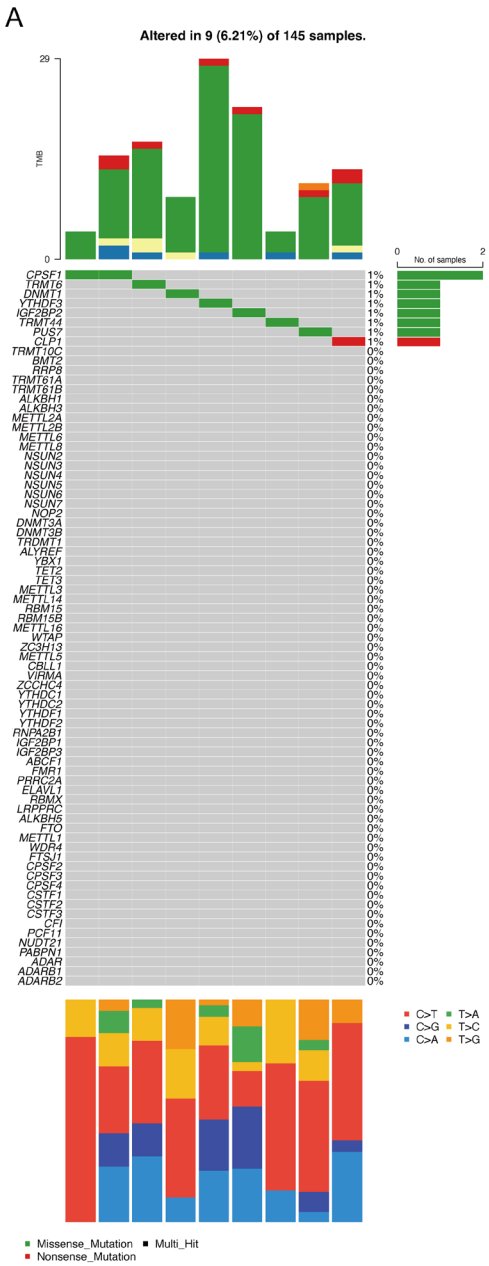

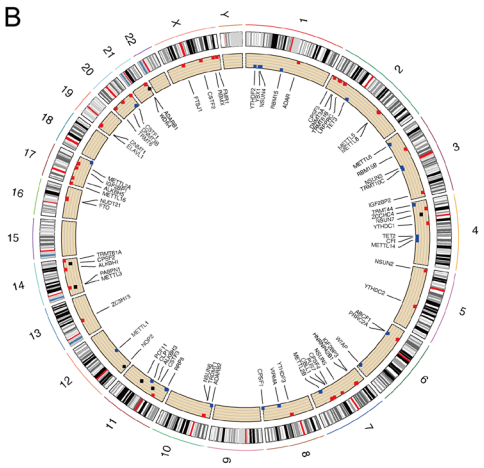

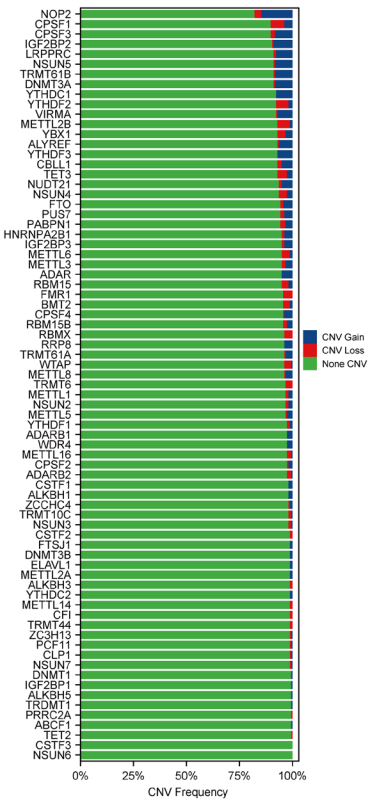

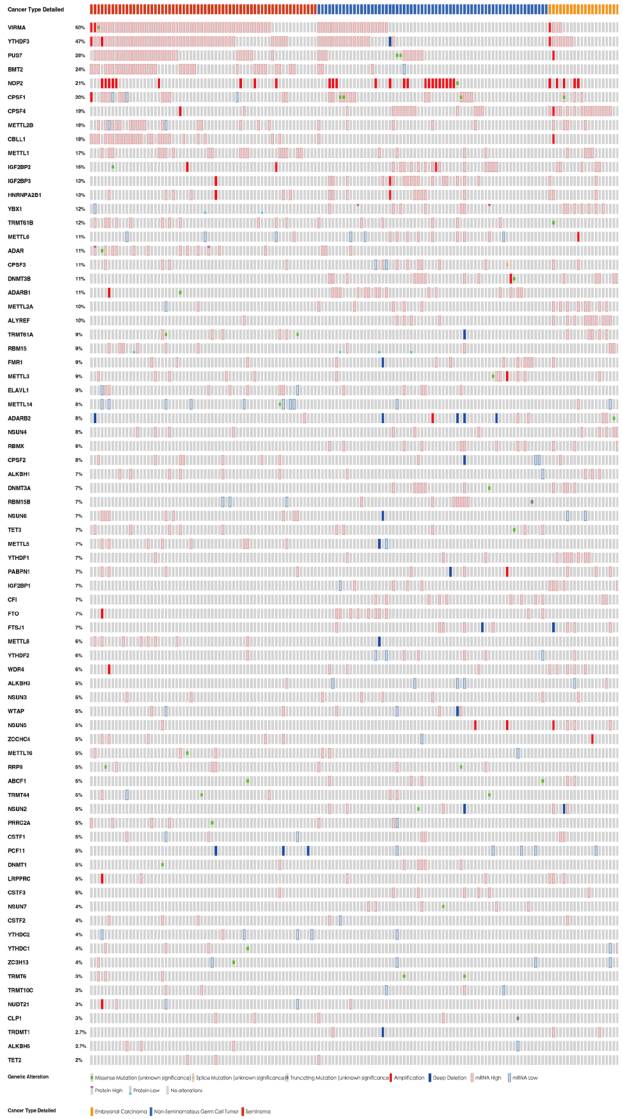

Figure S1. Landscape of the genetic alterations of RNA modification genes in TGCT patients. (A) 9 of 145 TGCT patients experienced genetic alterations of RNA modification genes, with a frequency of 6.21%. (B) The location of CNV alteration of RNA modification genes on chromosomes. (C) The overview mutation landscape of RNA modification genes in cBioPortal database. (D) The CNV mutation frequency of RNA modification genes. The column represented the percentage of alteration frequency.

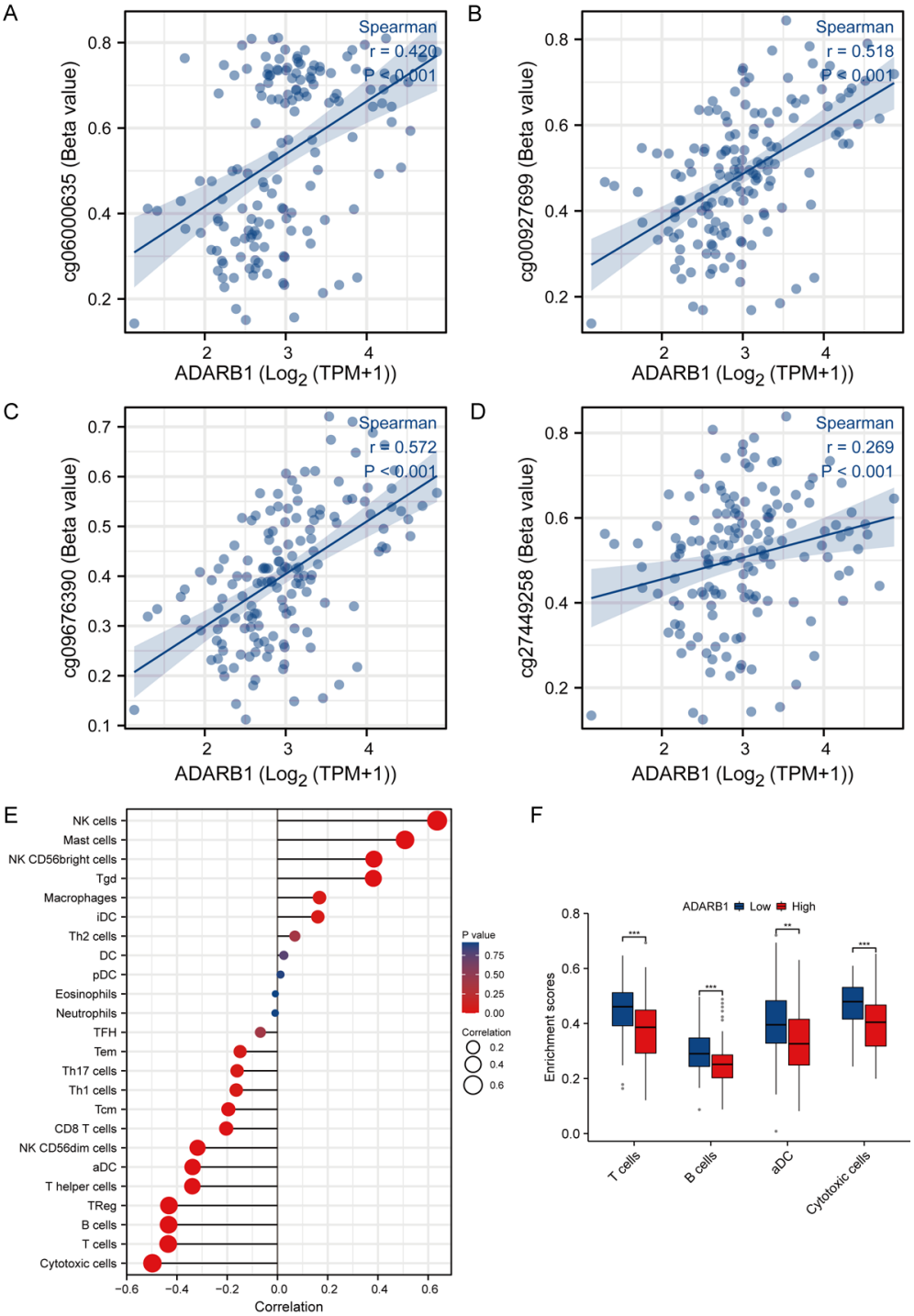

Figure S2. DNA methylation and immune cell infiltration of ADARB1 in TGCT patients. (A-D) Correlation analysis of ADARB1 and different DNA methylation sites, including cg06000635 (A); cg00927699 (B); cg09676390 (C) and cg27449258 (D). (E) Correlation analysis of ADARB1 and immune cell infiltration among tumor microenvironment. (F) Different immune cell infiltration characteristics among ADARB1-high and ADARB1-low subgroups.